NITRATE REDUCTASE STRUCTURE, FUNCTION AND REGULATION: Bridging the Gap between Biochemistry and Physiology

Wilbur H. Campbell

Phytotechnology Research Center and Department of Biological Sciences, Michigan Technological University, Houghton, Michigan 49931-1295; e-mail: wcampbel@mtu.edu

KEY WORDS: enzymology, 3-D structure, site-directed mutagenesis, molybdopterin cofactor, regulation, protein phosphorylation, 14-3-3 binding protein

ABSTRACT

Nitrate reductase (NR; EC 1.6.6.1-3) catalyzes NAD(P)H reduction of nitrate to nitrite. NR serves plants, algae, and fungi as a central point for integration of metabolism by governing flux of reduced nitrogen by several regulatory mechanisms. The NR monomer is composed of a ∼100-kD polypeptide and one each of FAD, heme-iron, and molybdenum-molybdopterin (Mo-MPT). NR has eight sequence segments: (*a*) *N*-terminal "acidic" region; (*b*) Mo-MPT domain with nitrate-reducing active site; (*c*) interface domain; (*d*) Hinge 1 containing serine phosphorylated in reversible activity regulation with inhibition by 14-3-3 binding protein; (*e*) cytochrome b domain; (*f*) Hinge 2; (*g*) FAD domain; and (*h*) NAD(P)H domain. The cytochrome b reductase fragment contains the active site where NAD(P)H transfers electrons to FAD. A complete three-dimensional dimeric NR structure model was built from structures of sulfite oxidase and cytochrome b reductase. Key active site residues have been investigated. NR structure, function, and regulation are now becoming understood.

CONTENTS

INTRODUCTION

Eukaryotic assimilatory nitrate reductase (NR) catalyzes the following reaction:

$$NO_3^- + NADH \rightarrow NO_2^- + NAD^+ + OH^-$$

$$\Delta G = -34.2\,\text{kcal/mol}\,(-143\,\text{kJ/mol}); \Delta E = 0.74\,\text{V}$$

With such a large negative free energy—under standard conditions, reduction of nitrate to nitrite by pyridine nucleotides is, for all practical purposes, an irreversible reaction. NADH-specific NR forms (EC 1.6.6.1) exist in higher plants and algae; NAD(P)H-bispecific forms (EC 1.6.6.2) are found in higher plants, algae, and fungi; and NADPH-specific forms (EC 1.6.6.3) are found in fungi. NR catalyzes the first step of nitrate assimilation in all these organisms, which appears to be a rate-limiting process in acquisition of nitrogen in most cases. Since nitrate is the most significant source of nitrogen in crop plants, understanding the role of NR in higher plants has potential economic importance, especially in light of recent studies illuminating the enzyme as one focal point for integration of control of carbon and nitrogen metabolism. With nitrate triggering and NR responding to metabolic changes in plants, the literature on nitrate and NR is vast, and nitrate metabolism and NR in plants have been reviewed from many points of view over the past few years (9, 11, 12, 18, 19, 37, 39, 62, 78, 81, 87, 92, 93). The intent here is to focus on the biochemical aspects of NR and its regulation, with the emphasis on higher plant metabolism; this brings together many threads in plant physiology with our current understanding of NR structure and function.

    Recent advancement of NR biochemistry has been dominated by molecular biology for over ten years. From the large number of NR cDNAs and genomic DNAs cloned and sequenced, a huge database of NR-deduced amino acid
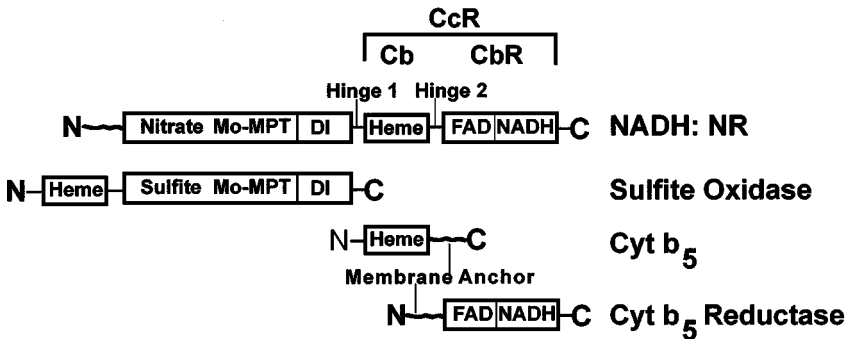
a
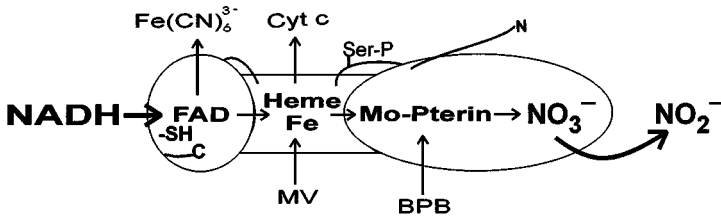
b

Figure 1 Nitrate reductase models. (*a*) Functional model of the enzyme; MV, methyl viologen; BPB, reduced bromphenol blue. (*b*) Sequence model of the enzyme; DI, dimer interface.

sequences has been produced (11, 18, 81, 93). This information on NR has confirmed many earlier discoveries in NR biochemistry and also led to new ones. To a great extent, the culmination of this combined biochemical knowledge is embodied in the two models depicted in Figure 1. The complex problem of studying the structure and function of NR has been simplified by expression of functional recombinant fragments of the enzyme. This resulted in the first 3-D structure information for NR (11, 56). With the problem of lack of expression of the holo-NR in recombinant form now overcome (28, 95, 96), NR biochemical discovery will return to its roots, and detailed analysis of the complete enzyme can begin in earnest. Molecular biology has been integrated as a tool to study NR biochemistry both as a mechanism to generate the large amounts of enzyme needed for the detailed studies of structure and function, and a means

to produce the site-directed mutants that permit investigations not possible with studies limited to natural forms.

STRUCTURAL CHARACTERISTICS

Polypeptide Sequence

The early studies of NR identified it as a flavoprotein containing a heme-Fe and molybdenum complexed with a unique pterin or molybdopterin (Figure 1*a*). NR was shown to catalyze a number of partial reactions including a dehydrogenase functionality typified by NADH-dependent reduction of ferricyanide and mammalian cytochrome c, which could be inhibited at a sensitive thiol protected by NADH (11, 12, 18, 81, 94). It was also shown that nitrate reduction could be driven with reduced flavins, methyl viologen, and bromphenol blue, which could be inhibited independently from the dehydrogenase function. Subsequently, it was deduced that all these reactions catalyzed by NR, including the natural NADH/NADPH-driven nitrate reduction, were best understood by viewing the enzyme as a redox system with an internal electron transfer chain. The enzyme is a homodimer composed of two identical ~100-kD subunits, each containing one equivalent of flavin adenine dinucleotide (FAD), heme-Fe, and Mo-molybdopterin (Mo-MPT). However, the amino acid sequence of the NR polypeptide was not revealed until the enzyme was cloned (11, 12, 18–20, 78, 81, 94). There are now more than 40 NR sequences in GenBank consisting of enzyme forms from higher plants, algae, and fungi and this number is growing every year. Comparison of NR sequences with those of known proteins and enzymes readily reveals conserved regions with similarity to a unique set of proteins (Figure 1*b*). The *Arabidopsis* NIA2 (hereafter called AtNR2), which contains 917 amino acid residues and has a molecular weight of 102,844 (20; GenBank Accession number J03240; Swiss Protein P11035), is a representative model for NR, and the numerical positions of the distinct sequence regions of AtNR2 are identified in Table 1. More recent data on the 3-D structure of NR, once thought to contain only 3 domains, indicate that it actually contains 5 structurally distinct domains: Mo-MPT, dimer interface, cytochrome b (Cb), FAD, and NADH (Figure 1*b*). When the FAD and NADH domains are combined, the cytochrome b reductase fragment (CbR) is formed, and when the Cb domain is joined to CbR, it is called the cytochrome c reductase fragment (CcR), as shown in Figure 1*b*. Three sequence regions with no similarity to another protein and varying in sequence among NR forms are: (*a*) the N-terminal region, which is rich in acidic residues but is also quite short in some NR forms; (*b*) Hinge 1, which contains the site of protein phosphorylation—Ser534 in AtNR2 and a trypsin proteolytic site; and (*c*) Hinge 2, which also contains a proteinase site. Recently, an NR was cloned from a marine diatom, *Heterosigma*

Table 1 Key invariant residues in Arabidopsis NIA2 (GenBank Accession No. J03240)[a]

Domain/region	Span (# residues)	Invariant (# residues/%)	Key residues	Function
N-terminal	1–90 (90)	0/0.0	None	Regulatory/Stability
Mo-MPT	91–334 (244)	33/13.5	8	Nitrate reducing active site
			Arg144	Nitrate binding
			Hist146	MPT binding
			Cys191	Mo ligand
			Arg196	Nitrate binding
			His294	MPT binding
			Arg229	MPT binding
			Gly308	Mo $=$ O ligand
			Lys312	MPT binding
Dimer interface (DI)	335–490 (156)	10/6.4	2	Formation of stable dimer
			Glu360	Ionic bond at interface
			Lys399	Ionic bond at interface
Hinge 1	491–540 (50)	5/10.0	1	Regulatory
			Ser534	Phosphorylated
Cytochrome b (Cb)	541–620 (80)	10/12.5	2	Binds Heme-Fe
			His577	Heme-Fe ligand
			His600	Heme-Fe ligand
Hinge 2	621–660 (40)	0/0.0	None	Unknown
FAD	661–780 (120)	10/8.3	5	Binds FAD/active site
			Arg712	Binds FAD
			Tyr714	Binds FAD
			Gly745	Binds FAD
			Ser748	Binds FAD
			Lys 731	Binds NADH
NADH	781–917 (137)	9/6.6	3	Binds NADH/active site
			Gly794	Binds NADH
			Cys889	Active site
			Phe917	C-terminal

[a]See Figures 1*b* and 3.

akashiwo Raphidophyceae, which contains a 116-residue hemoglobin domain (bacterial or protozoan type) inserted between the Cb and FAD domains of an otherwise typical NR sequence (Y Nakamura & T Ikawa, personal communication). Thus, the *C*-terminal region of this NR is similar to a bacterial enzyme called flavohemoglobin, which is a combination of a hemoglobin and an NADH flavo-reductase with structural features in common with NR's CbR (25). Clearly, NR is built from modular units that have evolved independently

to some degree and are related to similar modular units existing in many modern enzymes and proteins. The CbR fragment of NR is most closely related to cytochrome b_5 reductase (66; EC 1.6.2.2), whereas NR's Cb is related to eukaryotic cytochrome b_5 (59), which is a redox partner of its reductase with both anchored in the endoplasmic reticulum, although soluble forms of these proteins also exist in mammalian systems (Figure 1*b*). The Mo-MPT and interface domains of NR are most closely related to sulfite dehydrogenase (EC 1.8.2.1), commonly called sulfite oxidase (SOX), which is a detoxification enzyme found in the intermembrane space of mitochondria where sulfite is reduced to sulfate by reduced cytochrome c (37, 51). SOX also contains a cytochrome b domain related to the Cb of NR.

## *Cofactors and Metal Ions*

NR contains three internal cofactors (FAD, heme, and MPT) and two metal ions (Fe and Mo) in each subunit (11, 12, 18, 77, 81, 94). During catalytic turnover, the FAD, Fe, and Mo cyclically are reduced and oxidized. Thus, NR exists in oxidized and reduced forms, with the 12 to 18 possible oxidized and reduced forms (3 states for FAD, 2 states for Fe, and either 2 or 3 states for Mo) having only transient existence in vivo. Redox potentials for FAD, heme-Fe, and Mo-MPT in holo-NR and its proteolytic or recombinant fragments are -272 to -287 mV, -123 to -174 mV, and -25 to $+15$ mV, respectively (4, 11, 37, 75, 76, 93, 94, 98). This redox pattern is consistent with a "downhill" flow of electrons within the enzyme from NADH with a redox potential of -320 mV to the nitrate-reducing active site, where nitrate is reduced with a redox potential of $+420$ mV. The potential of the FAD in recombinant CbR is shifted more positive by 22 to 70 mV when NAD^+ is present and also by ADP and other NAD^+ analogs (4, 75, 94, 98). Since ADP produces a similar shift of potential in FAD as NAD^+ and the impact of the inhibitors are related to the strength of binding to CbR (4), these effects are probably transmitted through a conformational change in the NADH domain by its contacts with the FAD domain of CbR. However, NAD^+ forms a charge-transfer complex with reduced FAD with unique spectral properties (75, 94, 98). Site-directed mutagenesis of residues in either the FAD or NADH domains of CbR alters the redox potential of the FAD, but mutation of the active site Cys (Cys889 in AtNR2) does not affect the magnitude of the redox potential shift to a significant extent when NAD^+ is present (4, 75, 98). The redox potential of the heme-Fe in the enzyme's Cb depends greatly on the form of NR used for the measurement. Recombinant Cb or Cb fused to CbR in a CcR fragment has a redox potential of $+15$ or $+16$ mV, and a Cb fragment with an *N*-terminal extension containing the dimer interface domain and Hinge 1 yields -28 mV, whereas holo-NR's Cb is poised at about -100 to -200 mV (11, 13, 14, 76, 93, 94, 102). Thus,

the Mo-MPT and interface domains of NR on the *N*-terminal side of the Cb interact with it to make the heme-Fe redox potential more negative by more than 100 mV. Mammalian cytochrome b_5 has a potential of $+5$ mV, whereas heme-Fe in flavocytochrome b_2 has a potential of -31 mV in the recombinantly expressed Cb fragment and $+5$ mV in the holoenzyme (7, 50, 79). The conclusion is that while the conformation of the heme-Fe in NR's Cb, as recently shown by NMR (102), is similar to that in cytochrome b_5 (59), the environment of the charged residues in the Cb domain in relation to the *N*-terminal domains of NR significantly influences the redox potential of heme-Fe in Cb. Perturbation of the interface between the Cb and *N*-terminal domains may therefore be a mechanism for "redox" regulation of NR activity.

Molybdopterin is a unique cofactor in NR found in only three other enzymes in plants, xanthine dehydrogenase, aldehyde oxidase, and SOX, with some question remaining about the existence of SOX in plants (62). These enzymes have a 31-amino acid residue sequence motif characteristic of eukaryotic molybdopterin oxidoreductases (40), containing the invariant Cys residue involved in binding to Mo-MPT, which is Cys191 in AtNR2 (20, 96). NR and SOX have a similar "oxy" form of Mo-MPT, whereas the other eukaryotic enzymes have a Mo-MPT with a terminal sulfur (37, 47, 51, 62). Prokaryotes contain a conjugated form of molybdopterin where MPT is linked to a nucleotide (37, 47). Although the chemical structure of the core of MPT was worked out some years ago by Johnson et al (47), 3-D structures of the cofactor in enzymes have revealed that the bicyclic pterin ring is fused to the side chain (37, 51, 62), presumably after the MPT is bound to the protein (Figure 2*a*). In the 3-D structure of chicken liver SOX (51), the "X" in MPT is the thiol side chain of Cys-185 (Figure 2*b*, *c*). This structure for Mo-MPT in SOX is consistent with X-ray absorption spectroscopy of human SOX where 3 S and 2 O atoms were liganded to the Mo (29, 30). Recent X-ray absorption spectroscopic analysis of NR reveals the same complement of ligands to Mo with bond distances similar to SOX (G George, J Mertens & WH Campbell, unpublished results). These results provide evidence that the thiol of Cys191 of AtNR2 is indeed a ligand to Mo in the Mo-MPT enzyme complex and suggest that Mo-MPT in NR may have a conformation very similar to the cofactor in SOX. Biosynthesis of MPT from guanosine in plants has been analyzed in detail recently, and the involvement of at least 7 enzymes and proteins has been identified (62).

Functional Fragments and Domains

Cloning of NR and discovery of the linear arrangement of the sequence regions for apparent binding of the cofactors in the enzyme's primary structure were major advances in our understanding of NR biochemistry (Figure 1*b*). A number of studies, including mild proteolytic degradation experiments, had shown that

a

b

c
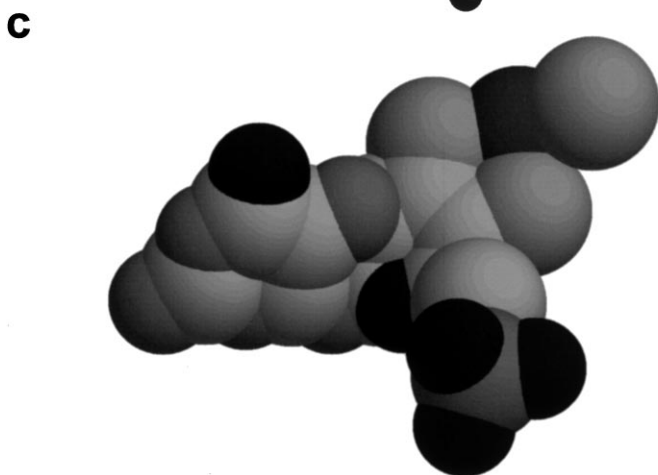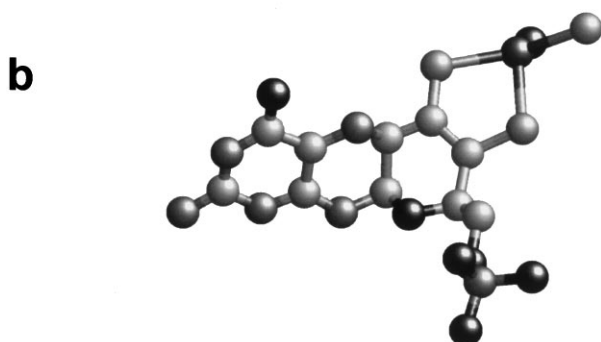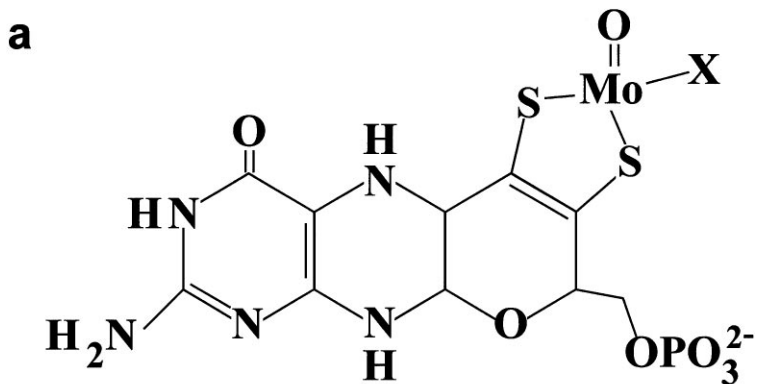
the cofactor binding fragments of NR, called "domains," represented functional subparts of the enzyme: a flavin-containing dehydrogenase fragment catalyzing either ferricyanide or cytochrome c reduction and the cytochrome b/Mo-MPT fragment catalyzing dye-dependent nitrate reduction (see Figure 1*a*). These experiments were the direct precursors of the recombinant expression of functional fragments of NR. The first recombinant fragments to be expressed were corn NR's CbR with NADH: ferricyanide reductase activity and *Chlorella* NR's Cb domain, which were expressed in *Escherichia coli* (11, 13, 14, 43). Subsequently, a fragment of NR containing Cb and CbR was expressed as a CcR fragment (11, 76, 90). A combined fragment of a "synthetic" rat cytochrome b5 and spinach NR's CbR was also expressed with cytochrome c reductase activity (73, 74, 98). These experiments unequivocally established that NR is built from modular units with stable structural integrity and catalytic functionality for partial reactions similar to the holo-NR. However, the Mo-containing fragment of NR has not been expressed as a recombinant independent fragment of the enzyme with functionality, but the holo-NR has now been expressed in active form in *Pichia pastoris*, a methylotrophic yeast (95, 96). NR of plants, algae, and fungi has also been expressed in recombinant systems where the NR gene is transformed into a NR-deficient mutant (21, 28, 33, 53, 68, 82–85). Finally and most recently, an extended form of the CcR fragment of corn NR with the putative dimer interface domain, called CcR-plus, has been expressed in *P. pastoris* and purified as an active cytochrome c reductase with a polypeptide size of 65 kD, which helps establish that the interface domain of NR is a structurally stable entity (JA Mertens & WH Campbell, unpublished results).

The CbR fragment of corn NR was crystallized and the 3-D structure determined by X-ray diffraction analysis (11, 56). The structure of CbR is composed of two domains: one for binding FAD and one for binding NADH. These results established NR's CbR as a member of the FNR structure family of flavoenzymes, which is named for ferredoxin NADP$^+$ reductase (6, 49). The interesting feature of this family of enzymes is that its members have little sequence similarity, sharing only a few key sequence motifs, while having a very similar conformation in their FNR-like fragment (17, 44, 49). Structures of many FNR family members have been determined, including spinach and *Anabaena* ferredoxin-NADP$^+$ reductases, corn NR's CbR, rat cytochrome P-450 reductase, pig

←——————————————————————————————————

Figure 2 Structure of the molybdopterin cofactor of nitrate reductase. (*a*) Chemical structure of molybdopterin when bound to a Mo-containing enzyme where X is an undefined ligand atom. (*b*) Ball and stick model of the structure of the Mo-molybdopterin complex of sulfite oxidase with the thiol sulfur atom of Cys185 shown as "X" (51). (*c*) Space-filling model of sulfite oxidase Mo-molybdopterin (51).

cytochrome b_5 reductase, *Pseudomonas cepacia* phthalate dioxygenase reductase, *Alcaligenes eutrophus* flavohemoglobin, and *E. coli* flavodoxin reductase (6, 11, 17, 25, 46, 49, 56, 57, 66, 88, 101). The flavin-binding domains of these enzymes are 6-stranded anti-parallel β-barrels with a single α-helix. The pyridine nucleotide-binding domains are 5- or 6-stranded parallel β-sheets, which have similarity in conformation to the classic Rossman dinucleotide fold found in many dehydrogenases (49, 79). The relative position of the two nucleotide binding domains differs among these enzymes and this difference appears to be related to the electron-acceptor for the flavin, which is either another redox center within the same protein (heme-Fe, iron-sulfur, or another flavin) or in another protein (heme-Fe, ferredoxin, or flavodoxin). In corn NR's CbR, the active site sits between these two domains where two electrons are transferred from NADH to FAD. A structure for the complex of ADP with CbR has also been reported that identified part of the NADH binding site (57). In addition, an atom-replacement model, using mammalian cytochrome b_5 as a guide (59), was made for the cytochrome b domain of corn NR and docked to the CbR structure to generate a model for the CcR fragment of NR (57). Most recently, an apo-CbR (without bound FAD) complex with NAD^+ has been obtained, as well as a native CbR form with NAD^+ bound (54). Unfortunately, none of the NAD^+ complexes with CbR appear to show the cofactor bound into the active site with the nicotinamide portion positioned for electron transfer to FAD. An active site mutant was generated for corn CbR where the only invariant Cys in this sequence region of NR was replaced by Ser (called C242S), and it was shown by kinetic analysis that NADH bound normally to this mutant but that the transfer of electrons from NADH to FAD was greatly impaired (11, 24, 75). The 3-D model of the C242S mutant of CbR showed that the hydroxyl side chain of the replacement Ser hydrogen-bonded to the protein backbone, leaving a void in the active site where the SH group of the Cys in the wild-type enzyme normally sat and directed the positioning of the NADH for optimum electron transfer to the FAD (11, 57). A similar site-directed mutant was recently reported for the CbR fragment of spinach NR, and kinetic and redox potential analyses were carried out (4, 74, 98). These results identify this Cys residue (Cys889 in AtNR2) as the inhibitor-sensitive thiol of NR (see Figure 1*a*) and demonstrate that its role is in assisting electron transfer and not binding of NADH, as originally thought (9, 11, 12, 24, 75).

Working 3-D Structure Model of Holo-Nitrate Reductase

Crystallization of holo-NR has not yet been successful despite intensive efforts. Recently, Kisker et al (51) determined the 3-D structure of chicken liver SOX, which is the only known protein with a high degree of sequence similarity

to the Mo-MPT-binding region of NR (11, 12, 18, 51, 81, 94). Since SOX and NR Mo-MPT fragments have almost 50% identity in sequence, a good quality atom replacement model for this region of NR has been generated using AtNR2 and the coordinates for SOX (WH Campbell & C Kisker, unpublished results). Furthermore, since SOX is a dimer like NR and has a cytochrome b domain with similarity to NR's Cb, it is possible to "dock" the CcR model of corn NR (57) in relation to the Mo-MPT and dimer interface domains to generate a complete working model for dimeric holo-NR (Figure 3: see color section at the end of the volume). The structure of the SOX/NR monomeric unit can be viewed thus: residues 2 to 84 = Cb domain with a 3-stranded anti-parallel β-sheet and 6 α-helixes; residues 96 to 323 = Mo-MPT/sulfite domain with 13 β-strands in 3 β-sheets and 9 α-helixes; and residues 324 to 466 = interface domain with 7-β strands in 2 β-sheets with similarity to the immunoglobulin structural family (51). The only difference between SOX and NR being the Cb domain in NR is *C-terminal* to the interface domain (Figure 1*b*). The contacts between the SOX monomers are composed almost entirely of residues from the interface domains bonding by hydrogen and ionic bonds (51). A single Mop-terin cofactor is buried in the Mo-MPT domain with hydrogen bonds formed by residues that are conserved in both SOX and NR, indicating the cofactor may have the same conformation in the two enzymes (see Figure 2*b*, *c*). In addition, sulfite or sulfate was found near the Mo-MPT with the anion liganded to three positively charged residues (Arg-138, Arg-190, and Arg-450), which appear to form the substrate binding site with Trp-204, Tyr-322, and Lys-200 also contributing (51). Only some of these residues are conserved in NR as Arg-144, Arg-196, Trp-210, and Lys-206 in AtNR2, which may form the nitrate-binding pocket. An interchain disulfide bond between the monomers of NR was found in a higher plant form but not in algal and fungal NR forms (45), although no potential Cys residue(s) for this functionality could be identified at the subunit interface in the working model of NR. Three regions of NR cannot be modeled from SOX, including the *N*-terminal "acidic" region, Hinge 1, and Hinge 2. However, the relative position of these parts of NR can be suggested from the positions of the *N*- and *C*-terminal residues of the domains lying on either side of these regions, which are illustrated schematically in Figure 3*b*. The schematic model also clarifies several features of the holo-NR working model, such as the relative positions of the FAD- and NADH-binding domains of CbR to the Cb, Mo-MPT, and interface domains. The CbR fragment, especially in the short linker region between its FAD and NADH domains, may actually have structural contacts with either the interface or Mo-MPT domains, or both, as well as with the Cb domain. Confirmation of these and other aspects of the structure of holo-NR awaits determination of the structure of the complete enzyme.

FUNCTIONAL CHARACTERISTICS

Reactions Catalyzed by Nitrate Reductase and Its Functional Fragments

The physiological function of NR is to catalyze pyridine nucleotide-dependent nitrate reduction as a component of the nitrogen-acquisition mechanism in higher plants, fungi, and algae. We suggested that NR could also participate in iron reduction in vivo since it catalyzes NADH ferric citrate reduction, but many other enzymes also catalyze this reaction in plants (9, 78). The only other NR catalytic reactions in vivo are with the alternate substrates, chlorate, bromate, and iodate, which yield chlorite, bromite, and iodide (iodite is unstable), respectively. Chlorate reduction is, of course, deadly for plants (chlorate has been used commercially as a defoliant and herbicide) unless they have no NR or nitrate transport system. This property has been a useful tool for obtaining mutant plants (18, 19, 81, 94, 99). Reduction of iodate by algal NR is a likely mechanism for altering the iodate-iodide balance in the ocean. NR is unusual since it is a soluble protein that catalyzes a redox reaction involving an electron transport chain and has physically separated active sites: one for NADH to reduce FAD at the beginning of the electron transport chain and one for reduced NR by the Mo-MPT to reduce nitrate (Figure 1*a*). NR resembles the mitochondrial electron transport chain since electrons from NADH can leave the enzyme to other acceptors (ferricyanide, cytochrome c, etc) besides nitrate, other electron donors (reduced dyes and flavins) can provide electrons for nitrate reduction, and part of the enzyme can be inhibited while leaving the other part functional (11, 12, 16, 81, 94). However, the large free energy available in NADH-linked nitrate reduction is not conserved unless NR is membrane bound, as it is in bacterial respiratory forms (5). Many claims have been advanced over the years for membrane-bound NR forms in higher plants and algae, but the "membrane" fraction was always small compared to the soluble NR level. In addition, there is no solid evidence proving the existence of membrane NR nor is there any explanation of how membrane-bound NR would function any differently than the soluble form.

The "artificial" partial reactions catalyzed by NR have been very useful in studying the biochemistry of the enzyme and understanding its catalytic mechanism. The partial reactions allowed the clear identification of NR proteolytic fragments as functional units of the enzyme and have been instrumental in characterizing the recombinant fragments of the enzyme. Basically, the fragments of NR with functionality in separate portions of the polypeptide proved that NR has two physically separated active sites, which helps explain its unusual steady-state kinetic mechanism. The kinetic model of NR is a two-site ping-pong type where NADH reduced the FAD at the first active site, and the

electrons are passed along the electron transport chain by the internal cytochrome b to the Mo-MPT where nitrate is reduced in the second active site (9, 11). A key concept in this mechanism is that NADH and NAD^+ bind to one active site in a mutually exclusive manner, while nitrate and nitrite act the same way at the other active site. Thus, nitrate can bind to the oxidized enzyme without impeding NR reduction by NADH, which may be important if the nitrate-reducing active site is buried deep in the Mo-MPT domain, as the sulfite reduction site is in the Mo-MPT domain of SOX (51). Although not completely accepted (94), the two-site ping-pong steady-state kinetic model for NR is the most logical description of the steady-state kinetics of NR. NR is a highly efficient catalyst with a turnover number of 200 s^{-1} and true K_m values of 1 to 5 μM for NADH and 20 to 40 μM for nitrate (4, 9, 24, 75, 76, 96, 97).

Pre-steady-state kinetic analysis of the complete NR reaction has not yet been carried out since the holo-enzyme was not available in sufficient amounts. Recombinant production of the CbR and CcR fragments has permitted analysis of the rates of reduction of CbR by NADH and transfer of electrons from reduced FAD to the heme-Fe in CcR (11, 75, 76). Rates of NADH reduction of FAD in CbR and CcR were 474 and 560 s^{-1}, respectively, at 10°C, which was used since the rates at 25°C were too fast to be evaluated by the available equipment. The Kd NADH was 3 μM for either CbR or CcR, which fits well with the K_m NADH for NR (75, 76). The steady-state kcat for NADH ferricyanide reduction catalyzed by CbR at 25°C is 1300 to 1400 s^{-1} (24, 74). Clearly, NADH reduction of NR is faster than overall turnover by a factor of 6 to 7, which indicates either internal electron transfer from $FADH_2$ to Mo-MPT by the cytochrome b or that the reduction of nitrate by Mo-MPT is the rate-limiting process in NR. Electron transfer from $FADH_2$ to heme-Fe in the CcR has a rate of 12 s^{-1} at 10°C (76), which is too slow to have any meaning in relation to electron transfer within holo-NR. This slow step in electron transfer within CcR was thought to be related to the release of NAD^+ from the active site after reduction of FAD and before electrons could move to the heme-Fe, which might also be a slow process in NR catalysis. In the structural model of CcR, the distance between FAD and heme-Fe is about 15 Å (57), whereas the distance between the heme-Fe and Mo-MPT in SOX is 32.3 Å (51). These long distances for electron transfer between the redox centers are surprising considering the rapid turnover rates of these enzymes.

Essential Amino Acid Residues for Functionality

When all the available NR sequences are compared with related proteins and enzymes in a multi-alignment, the number of invariant residues is reduced to ~77 from 917 in AtNR2, and this number can be further decreased to 21 specific

residues using other available information (Table 1). Of these key residues, only four have been studied using site-directed mutagenesis. For example, there are only two invariant Cys residues, Cys191 and Cys889, in AtNR2. Cys191 was replaced by Ser and Ala in AtNR2 and expressed in *P. pastoris*; although both mutants produced a complete NR polypeptide, neither was active (96). Cys191 corresponds to Cys185 of SOX, a known ligand to Mo in the enzyme's active site (see Figure 2*b*), which suggests that Cys191 is essential for NR activity since it must be present to bind to Mo for functionality of this redox center. A Ser replacement mutant of the SOX Mo-liganded Cys has also been generated; it lacks activity and also lacked the sulfur ligand to Mo when examined by X-ray absorption spectroscopy (29, 30, 51). AtNR2 Cys889 is equivalent to the invariant Cys in the CysGly motif of FNR family enzymes (11, 17, 43, 49, 56). Cys242 of corn CbR, equivalent to C889 in AtNR2, was replaced by Ser (called C242S) and the purified, recombinant enzyme fragment lost most of its ferricyanide reductase activity (24). A study of mutants of this invariant Cys in *Neurospora crassa* NADPH:NR also found that all substitutions at this position lost NADPH nitrate-reducing activity as well as ferricyanide reductase activity in a recombinant CbR fragment of this enzyme expressed in *E. coli* (33). Clearly, this Cys is not absolutely required for activity of NR, but its presence makes electron transfer from NADH to FAD much more efficient (24, 75). The role of Cys889 in NR appears to be to position NADH for efficient reduction of FAD. Using the recombinant *A. nidulans* NADPH:NR expression system, several key conserved residues of NR have been investigated using site-directed mutagenesis (28), including replacement of the invariant Cys in the Mo-MPT domain with Ala (C150A in *A. nidulans*) and one of the His ligands of the heme-Fe of the cytochrome b domain with Ala (H547A in *A. nidulans*). The C150A mutant lost all nitrate-reducing activities, whereas H547A lost only the NADPH and methyl viologen NR activities while retaining the bromphenol blue NR, which does not depend on a functional heme-Fe (11, 28, 81, 94). A His-ligand to the heme-Fe of tobacco NR was mutated to an Asn in an NR-deficient plant (63). These results are entirely consistent with the model of NR functionality presented in Figure 1*a*, where the thiol group shown near the FAD represents Cys889 of AtNR2.

Several other residues in the FAD domain of *N. crassa* NADPH:NR have been mutated in both the CbR fragment and holoenzyme (33). The most notable mutation was the substitution of Gly809 and Thr812 with Val and Ala, respectively, which resulted in loss of both NADPH NR and ferricyanide reductase activities. These residues correspond to residues Gly745 and Ser748 in AtNR2 and Gly95 and Thr98 in recombinant corn CbR. In the 3-D structure of CbR, Gly95 and Thr98 are shown to be involved in binding FAD, with the Gly serving a structural role and the Ser/Thr hydrogen bonded to the

pyrophosphate bridge in the middle of FAD (56, 57). Gly308 in AtNR2 was found to be mutated to Asp in a chlorate-resistant mutant plant and the NR was not only inactive but also not phosphorylated in vivo (52). This residue corresponds to Ala297 in SOX, which makes a polypeptide backbone hydrogen bond to the terminal oxygen of Mo in the active site (51). Substitution of Asp for Gly308 in AtNR2 could then abolish NR activity since the backbone might take a very different course in the mutant NR, but how this would preclude phosphorylation is less clear. Ser534 in AtNR2 has been identified as the site of phosphorylation of NR by replacement with Asp, which resulted in loss of inhibition of NR activity in an in vitro assay for regulation of NR (95). This residue in spinach NR (i.e. Ser543) has been studied extensively in relation to the protein kinase that catalyzes phosphorylation of NR and is discussed below. Obviously, Ser534 is not required for NR activity and is not even present in fungal and algal NR forms. Other nonessential, but key residues in NR, such as those at the interface between the two monomeric units of the dimer (Table 1), have not yet been studied. Several groups have investigated the *N*-terminal region of NR (53, 65, 68, 96), which is clearly not essential since it is virtually absent from some NR forms, and contains no invariant residues. These studies have focused on the role of this region in NR regulation and are discussed below.

Residues Determining Pyridine Nucleotide Specificity in NR

NR is unusual among oxidoreductases since it exists in NADH- and NADPH-specific forms as well as bispecific forms that accept electrons from either NADH or NADPH. Since bispecific NR forms were the first identified in soybeans and as secondary NR forms in monocots like corn, rice, and barley, they have fascinated investigators. Why do some plants have both NADH: and NAD(P)H:NR forms? How do bispecific NR forms differ from the more specific NADH: and NADPH:NR? The first question, which can also be asked for *Arabidopsis* with its two NADH:NR forms, is more physiological, and several answers have been found including tissue specificity and differential expression (16, 18, 19, 78, 81, 94). In soybean, the pH 6.5 NAD(P)H:NR is constitutively expressed without nitrate present, which suggests that this enzyme is involved in another plant process besides nitrogen acquisition. In fact, this NR also catalyzes reduction of nitrite to NOx gases, but this process has never been studied in detail nor is it obvious what benefit it would be to the plant unless NOx is a hormone like it is in animals (9). Corn seedlings appear to express three forms of NR:NADH-specific, NAD(P)H-bispecific with similarity to barley, and a unique NAD(P)H-bispecific with some similarity to green algal NR since it lacks the regulatory Ser found in Hinge 1 of all other known higher plant NR

forms (3, 11, 78). The second question can be dealt with as a structural problem and investigated by sequence comparisons and structural determinations. The general conclusion is that NAD(P)H:NR forms appear to be similar to NADH:NR forms except that the barley enzyme has a shorter *N*-terminal region and minor differences occur in the pyridine nucleotide binding domain (11, 12, 18, 81, 94). Antibodies that readily distinguish the NR forms in barley or corn have not yet been obtained.

Since the 3-D structures of spinach FNR with 2′, 5′ADP bound and corn CbR with ADP bound are known (6, 11, 17, 57), these can serve as models for the design of site-directed mutants of NR forms to alter pyridine nucleotide specificity. The pyridine nucleotide binding domain of FNR family enzymes is a parallel β-sheet with the loops at the ends of the β-strands providing the ligands for binding the cofactor. In FNR and CbR, the third β-strand is followed by a loop containing the residues involved with determining if NADPH or NADH will bind. The distinguishing feature is that FNR binds the 2′ phosphate of NADPH with a positively charged Ser-Arg immediately after the β-strand, whereas CbR binds the 2′ hydroxyl of NADH with a negatively charged Asp (6, 17, 57). Since a Ser-Arg pair of residues is found in *N. crassa* NADPH:NR (Ser920-Arg921) in the same position as the Ser-Arg pair in FNR (43), mutants were prepared where Ala and Thr were substituted for Ser920, and Gly, Ala, and Thr for Arg921 (33). All these substitutions resulted in NR and CbR forms with NADPH nitrate and ferricyanide reducing activity that was decreased relative to wild type except for S920T, which had increased NR activity. To determine if the key residues in *N. crassa* NR are aligned like those in FNR or corn NR, mutant CbR forms were designed with Asp substituted for Ser920 and Ser and Thr for Arg921 and the mutant proteins purified for detailed kinetic analysis with both NADPH and NADH (91). Substituting Asp for Ser920 resulted in a virtual conversion of *N. crassa* CbR into an NADH-specific enzyme, whereas substitutions at Arg921 had no impact on specificity. Thus, it appeared that the 2′ phosphate of NADPH was not bound by Arg921, which indicates that the binding pocket in *N. crassa* NADPH:NR is more like that in NADH:NR than it is in FNR. An Arg more *C*-terminal (Arg932 in *N. crassa* NR), which is conserved in nearly all fungal NR forms and also found in monocot bispecific NR forms, is a candidate for supplying the positive charge in the binding site (91). Mutation of Arg932 did disrupt pyridine nucleotide binding but without showing a clear preference between NADPH and NADH (91). Birch NAD(P)H:NR is the only bispecific form to be investigated so far by site-directed mutagenesis, where residues in the binding site for the ribose and adenine of NADPH/NADH were altered (85). The Pro following the invariant Cys-Gly near the C terminus of NR (Pro891 in AtNR2), which is an Ala in birch NR and reverted to a Pro in the key mutant, favored NADH binding versus NADPH. The corresponding residue

Pro244 in corn CbR is indeed near the ribose of ADP and is well positioned to influence which cofactor binds to NR (57). Since other bispecific NR forms have not yet been studied in detail, the best explanation of their structural basis lies in the Ser or Lys residue found in the position immediately after the third β-strand of the pyridine nucleotide binding domain. If this is a negatively charged residue such as Glu854 in AtNR2 or Asp205 in corn CbR, then it appears that the negative charge on the $2'$ phosphate of NADPH is repelled and the preferred cofactor is NADH.

Glutathione reductase (EC 1.6.4.2) and isocitrate dehydrogenase (EC 1.1.1.42) are enzymes where NADPH/NADP$^+$-specific forms have been converted into NADH/NAD$^+$-specific forms by site-directed mutagenesis and detailed kinetic analysis carried out (15, 86). The 3-D structures of the wild-type and mutant forms have been compared to analyze the fine structure of their pyridine nucleotide binding sites (40, 63). In both cases, there are many differences between the NADH and NADPH binding sites, and consequently the conformation of the cofactor differs significantly when bound to the enzyme. This is reflected in the fact that about seven mutations were needed in each of these enzymes to convert from an NADPH- to NADH-specific form (15, 41, 64, 86), unlike NR where *N. crassa* CbR was converted from NADPH-specific to NADH-specific by a single mutation (91). Although the structure needs to be determined for NR, it appears that NADPH and NADH are bound to the enzyme in a very similar conformation, with the major difference being focused on the residues involved in binding the $2'$ phosphate of NADPH and $2'$ hydroxyl group of NADH. A similar conclusion was drawn in comparing the structures of spinach NADP$^+$ FNR and bacterial NADH phthalate dioxygenase reductase (17). The general conclusion is that only small changes in the fine structure of the pyridine nucleotide domain of NR are required to change from an NADH-specific form to an NADPH-specific form or perhaps even fewer to make a bispecific NR from a monospecific one, which may explain the existence of so many bispecific NR forms in nature.

REGULATION

Molecular Mechanisms for Regulation

NR catalytic flux or the total nitrate-reducing capacity of a plant system depends on: (*a*) availability of the substrates in the cytoplasm (steady-state concentrations of NAD(P)H and nitrate); (*b*) the level of functional NR (amount of NR polypeptide and availability of cofactors and metal ions—FAD, heme, Fe, Mo-MPT, and Mo); and (*c*) the activity level of the functional NR. Each process is regulated either directly or indirectly, and the overall level of nitrate reduction capacity is controlled in relation to overall plant metabolic level by metabolic

sensors and signal transduction pathways. Stitt and coworkers (82–84) have recently studied in detail these control systems in tobacco plants with the normal four copies of the NR gene, and they genetically manipulated plants with 0, 1, and 2 NR gene copies. The free Gln level and its ratio to free Glu, as well as the nitrate level, are probably the key metabolites governing the level of nitrate-reducing capacity in a plant (18, 81, 82, 94). When Gln levels are low and nitrate is available, NR level and nitrate-reducing capacity are boosted, whereas high Gln levels "throttle" nitrate reduction and decrease activity levels of NR. However, in transgenic plants where NR mRNA is expressed constitutively and posttranslational control is lost owing to deletion of the *N*-terminal region of NR, the control linked to the Gln/Glu balance is lost and nitrate-reducing capacity is controlled by NADH availability only (53, 68). In normal plants with optimum growth conditions and sufficient nitrate, the nitrate-reducing capacity is about two times greater than the plant needs, and NR activity levels cycle on a daily basis with low activity in the dark (82). Nitrate essentially acts as a hormone in plants by inducing functional NR and a host of other enzymes and proteins, perhaps including DNA regulatory proteins, involved in the metabolic response to the availability of a limiting nutrient, which includes changes in the root-to-shoot ratio and morphological changes such as root hair development (18, 78, 82–84). The expression of nitrate transporter genes are also induced by nitrate (18, 99). The degree of the plant response to nitrate depends on other environmental and genetic factors such as light and plant genotype, which influence NR and the other components of the nitrate metabolic mode. The response of NR to nitrate depends on a constitutively produced "nitrate-sensing" protein of unknown character, which presumably binds to regulatory regions in the NR gene and turns on expression of the NR mRNA (78). The nitrate box regulatory sequences in the promoter of the NR genes have been identified (42). Presumably, other regulatory boxes such as for light, tissue specificity, Gln/Glu balance, water and carbohydrate status, the photosynthesis rate of the plant, and other limiting conditions are present in the promoters of NR and related nitrate response genes (18, 78). These signals are integrated with the nitrate response by their specific DNA-binding proteins, which combine to influence the level of gene transcription by the strength of the initiation complex for binding RNA polymerase II to start sequences in the genes. While NR mRNA levels rise rapidly in response to nitrate treatment of plants and reach a steady-state level in a few hours (18, 19, 81, 94), in plants where nitrate levels cycle, NR mRNA levels also cycle (27, 78, 82). Efficiency of NR polypeptide translation may also be a site for regulation but this has not been carefully studied. NR polypeptide must be assisted in folding by various chaperones but none unique to NR has been identified. Although inhibition of heme biosynthesis blocks NR activity appearance, the small amounts of functional NR protein required

to meet the nitrate-reducing needs of plants probably require little change in the normal cellular production of FAD and heme-Fe. Molybdate is probably transported into plants by the phosphate transport system and is probably not limiting. MPT biosynthesis requires seven gene products, but these are constitutively expressed and probably not influenced by the presence of nitrate (62). Analysis of NR protein levels in plants displaying a daily cycle of NR activity has revealed that NR is degraded daily (9, 11, 82). In summary, the level of functional NR is controlled at the transcriptional level, with fully complemented NR rapidly formed by combination of the NR polypeptide with the required cofactors. Functional NR, however, has a short half-life and the protein is degraded by proteolytic attack, perhaps involving a specific NR proteinase although no ubiquitous enzyme of this type has been identified. Superimposed on the de novo synthesis and irreversible degradation of NR are reversible controls of the level of enzyme activity.

NR Phosphorylation and Inhibition by the 14-3-3 Binding Protein

Kaiser and coworkers (48) discovered through the use of physiological studies of the level of NR activity in plants that NR is probably regulated by protein phosphorylation and dephosphorylation. Subsequently, NR was demonstrated to be a phospho-protein with the phosphorylated NR level linked to inhibition of NR activity in the dark in leaves, which depends on the presence of divalent cations such as Ca^{2+} or Mg^{2+} (38, 58). NR protein kinases that depend on calcium for activity have been characterized (3, 22, 39, 65). The specific site of NR phosphorylation is Ser534 of AtNR2 (Ser543 in spinach NR), which is found in Hinge 1 of virtually all higher plant NR forms (3, 23, 95). The identity of the target Ser has been confirmed in AtNR2 by directed mutation to Asp, which eliminated NR inhibition with an in vitro ATP-dependent system, and in spinach NR by sequencing of the phosphopeptides isolated after tryptic digestion and from model peptide studies (3, 23, 39, 65, 95). The sequence context of the Ser targeted for phosphorylation is important for protein kinase recognition and can be summarized as Leu-Lys-(Lys/Arg)-(Ser/Thr)-(Val/Ile/Ala)-target Ser-(Thr/Ser)-Pro-Phe-Met (3, 39). The reactivation of NR in the light depends on a type 2A protein phosphatase (inhibited by microcystin and okadaic acid), which catalyzes dephosphorylation of NR (38, 39, 58, 65). This apparently straightforward reversible regulatory mechanism for NR activity is complicated by the fact that highly purified NR is not inhibited by phosphorylation in vitro in the presence or absence of Mg^{2+} (39). This led to the discovery of an inhibitor protein in the extracts used to supply protein kinase activity, which has been identified as the widespread binding protein called 14-3-3 (2, 26, 39, 65, 87). The 3-D structure of mammalian 14-3-3 proteins has

been determined; it contains nine α-helices and is a dimer with two binding grooves about 30 Å apart (55, 103). Complexes of 14-3-3 proteins bound with target peptides containing the sequence Arg-Xxx-Xxx-Ser(P)-Xxx-Pro have been analyzed; these show that the phosphate is bound to two Arg and a Lys residue in the binding groove on one side whereas the other binds hydrophobic residues of the target sequence (71). This sequence is similar to that required for protein kinase recognition of higher plant NR except that the initial Arg is often a Lys in NR. In addition, other unique sequences with a negative charge in place of the phospho-Ser can also bind to the groove in 14-3-3 (71). Since NR from which the *N*-terminal highly acidic region has been deleted does not bind 14-3-3 proteins as well as native NR (53, 65, 68), the existence of a secondary binding site for 14-3-3 in this region is possible and it might not require phosphorylation for binding. Since fusicoccin also binds to 14-3-3, this fungal toxin can reverse the inactivation of NR by the binding protein (65, 87). To summarize reversible regulation, the NR protein must be phosphorylated by Mg-ATP at the unique Ser in Hinge 1 as catalyzed by a "specific" NR protein kinase; then in the presence of Mg^{2+}, a binding protein called 14-3-3, which is already present in the cytoplasm, binds to phospho-NR and inhibits NR activity. The binding of 14-3-3 to phospho-NR appears to block electron flow from the Cb domain to the Mo-MPT by an unknown mechanism (38, 39). Since the 14-3-3 binding protein appears to bind in a region where the dimer interface and Mo-MPT domains meet the Cb domain (see Figure 3*b*), the inhibition may be due to modulation of the redox potential of the heme-Fe, which is altered by disturbance in this region.

PRACTICAL APPLICATIONS

The Nitrate Pollution Problem

By the 1970s, the accumulation of nitrate in some surface and groundwaters of the United States, Canada, and Europe had become a serious enough threat to human health for most countries to adopt a Maximum Contaminant Limit (MCL) for potable water (36, 67, 92). In the United States, the MCLs for nitrate as 10 ppm nitrate-N and nitrite as 1 ppm nitrite-N were set by the Clean Water and Safe Drinking Water Acts of 1974. The immediate threat posed by high concentrations of nitrate in drinking water is methemoglobinemia or blue-baby syndrome, caused by strong binding of nitrite to hemoglobin and oxidation of the iron center, which is more serious in infants, since fetal hemoglobin binds nitrite more strongly and can result in death. The linkage between other human health risks such as cancer and long-term exposure to high nitrate concentrations in drinking water are not well enough documented to justify further restriction of the nitrate MCL, which already takes about 10% of the potable water in the

United States out of the useable pool (36, 67). Nitrate pollution is probably caused by agricultural practices whereby excess N is applied to fields to maximize crop yield and animal wastes are released into the environment without having to undergo a tertiary process to remove nutrients. Industrial processes and air pollution, especially from automobile exhaust, also contribute significantly to nitrate pollution (36, 72, 92, 100). One initiative to control the use of excess fertilizer is the USDA's nitrate leaching and economic analysis package (NLEAP) computer program. How to balance the need for increased crop production with the control of pollution caused by underutilization of applied nutrients is an active area of research (60, 69, 89). Nevertheless, nitrate/nitrogen and other nutrient pollution has become a major ecological problem worldwide (92, 100). The increase in toxic algal blooms in many coastal waters, the "dead zone" in the Gulf of Mexico along the southern US coastline, and the massive fish kills in American estuaries often accompanied by toxic microalgae such as *Pfiesteria piscicida* (70) are illustrations in point. Although the causes of ecosystem changes in these complex systems are difficult to pinpoint, nutrient runoff is of growing concern worldwide.

Nitrate Reductase as an Environmental Biotechnology Tool

Regulations to monitor nitrate usage require a reliable method to detect and quantify nitrate in water and soil. Although methods for quantification of nitrate based on NR-driven reduction to nitrite and colorimetric nitrite analysis were described many years ago, chemical reductants such as cadmium and zinc are the most commonly used commercially (8). The availability of stable preparations of NR that can be shipped at room temperature has promoted the development of NR-based commercial nitrate detection tests (8). Nitrate testing based on NR is a less polluting alternative to tests based on toxic heavy metals and has become a standard in biomedical research where nitrate and nitrite are often monitored as indicators of nitric oxide production (8, 32, 34, 35). Nitrate must also be monitored in surface and ground waters on a real-time basis. Devices based on chemical reduction of nitrate have been described, but none has yet been widely adopted, and nitrate biosensors based on NR have attracted attention (1, 32). An optical method using immobilized NR to detect nitrate has been developed (1). Recently, a nitrate electrode was developed based on corn leaf NR, where electrons are directly supplied to the enzyme for nitrate reduction by an electrode coated with methyl viologen. It has the capability to quantify nitrate in fertilizer solutions (32). The rapid advances made in using enzymes in other biosensors such as those based on glucose oxidase for monitoring blood glucose promise the early advent of a commercial nitrate biosensor based on NR. Methods to remove nitrate from potable water would be a solution for many communities and individuals where nitrate

pollution has contaminated their drinking water source. Nitrate is one of the most soluble anions and is difficult to remove by physical processes such as ion-exchange; although reverse osmosis is effective in removing nitrate, it is expensive. Furthermore, these removal methods concentrate the nitrate, which presents an additional significant waste-disposal problem. A better approach is to use denitrification, especially where the final product is environmentally benign dinitrogen gas. Denitrification can be accomplished by microorganisms (5), but the process can be slow and requires additional purification of the potable water. An alternative is to use an enzyme-based system with a combination of NR and bacterial denitrification enzymes (61). In the enzyme denitrification reactor, the reducing power was supplied to the immobilized enzymes by direct electric current through electron-carrying dyes, which resulted in complete removal of nitrate as dinitrogen with no additions to the water. This approach can be used for potable water at the point-of-use and generates no waste-disposal problem. The application of recombinant DNA technology to the production of NR and bacterial denitrification enzymes may make enzyme reactors for treating nitrate-polluted water commercially available. Clearly, basic research on NR has helped to advance the applications of this unique enzyme to address the nitrate pollution problem and genetically engineered plants may well promote more efficient use of N-fertilizers and thus reduce or prevent the pollution attributable to the application of excess nutrients.

EXPECTED DEVELOPMENTS

Within the next few years elucidation of a 3-D structure for plant holo-NR will guide its future study. Better understanding of the electron transfer process within NR is on the horizon, as is the identification of the rate-limiting process in nitrate reduction catalyzed by pyridine nucleotide-dependent NR. More detailed studies of various forms of NR including the unusual bispecific forms should provide a clearer understanding of pyridine nucleotide specificity. A better understanding of how the 14-3-3 binding protein inhibits phospho NR in higher plants and description of the details of a 3-D structural complex between phospho NR and 14-3-3 will be important in delineating the mechanism underlying regulation. Finally, more information is needed on how the nitrate signal is transmitted in plants and the character of DNA regulatory proteins that bind to the nitrate box in nitrate response genes. Considerable progress has been made recently in understanding the process of MPT biosynthesis, and the insertion of Mo-MPT into NR and related enzymes will surely be a focus of future research. Ultimately, validation of the public investment in basic research on NR may come in the form of commercial devices for monitoring nitrate levels in real-time and enzyme reactors for removing nitrate from water.

Visit the *Annual Reviews home page* at
http://www.AnnualReviews.org

Literature Cited

1. Aylott JW, Richardson DJ, Russell DA. 1997. Optical biosensing of nitrate ions using a sol-gel immobilized nitrate reductase. *Analyst* 122:77–80

2. Bachmann M, Huber JL, Liao PC, Gage DA, Huber SC. 1996. The inhibitor protein of phosphorylated nitrate reductase from spinach. *Spinacia oleracea* leaves is a 14-3-3 protein. *FEBS Lett.* 387:127–31

3. Bachmann M, Shiraishi N, Campbell WH, Yoo BC, Harmon AC, et al. 1996. Identification of the major regulatory site as Ser-543 in spinach leaf nitrate reductase and its phosphorylation by a Ca^{2+}-dependent protein kinase in vitro. *Plant Cell* 8:505–17

4. Barber MJ, Trimboli AJ, Nomikos S, Smith ET. 1997. Direct electrochemistry of the flavin domain of assimilatory nitrate reductase: effects of NAD^+ and NAD^+ analogs. *Arch. Biochem. Biophys.* 345:88–96

5. Berks BC, Ferguson SJ, Moir JW, Richardson DJ. 1995. Enzymes and associated electron transport systems that catalyse the respiratory reduction of nitrogen oxides and oxyanions. *Biochim. Biophys. Acta* 1232:97–173

6. Bruns CM, Karplus PA. 1995. Refined crystal structure of spinach ferredoxin reductase at 1.7 Å resolution: oxidized, reduced and 2′-phospho-5′-AMP bound states. *J. Mol. Biol.* 247:125–45

7. Brunt CE, Cox MC, Thurgood AG, Moore GR, Reid GA, et al. 1992. Isolation and characterization of the cytochrome domain of flavocytochrome b$_2$ expressed independently in *Escherichia coli*. *Biochem. J.* 283:87–90

8. Campbell ER, Corrigan JS, Campbell WH. 1997. Field determination of nitrate using nitrate reductase. In *Proc. Symp. Field Anal. Methods Hazard. Wastes Toxic Chem.*, ed. E Koglin, pp. 851–60. Pittsburgh: Air & Waste Manage. Assoc.

9. Campbell WH. 1989. Structure and synthesis of higher plant nitrate reductase. See Ref. 102a, pp. 123–54

10. Campbell WH. 1992. Expression in *Escherichia coli* of cytochrome c reductase activity from a maize NADH:nitrate reductase cDNA. *Plant Physiol.* 99:693–99

11. Campbell WH. 1996. Nitrate reductase biochemistry comes of age. *Plant Physiol.* 111:355–61

12. Campbell WH, Kinghorn JR. 1990. Functional domains of assimilatory nitrate reductases and nitrite reductases. *Trends Biochem. Sci.* 15:315–19

13. Cannons AC, Barber MJ, Solomonson LP. 1993. Expression and characterization of the heme-binding domain of *Chlorella* nitrate reductase. *J. Biol. Chem.* 268:3268–71

14. Cannons AC, Iida N, Solomonson LP. 1991. Expression of a cDNA clone encoding the haem-binding domain of *Chlorella* nitrate reductase. *Biochem. J.* 278:203–9

15. Chen R, Greer A, Dean AM. 1995. A highly active decarboxylating dehydrogenase with rationally inverted coenzyme specificity. *Proc. Natl. Acad. Sci. USA* 92:11666–70

16. Cheng C-L, Acedo GN, Dewdney J, Goodman HM, Conkling MA. 1991. Differential expression of the two Arabidopsis nitrate reductase genes. *Plant Physiol.* 96:275–79

17. Correll CC, Ludwig ML, Bruns C, Karplus PA. 1993. Structural prototypes for an extended family of flavoprotein reductases: comparison of phthalate dioxygenase reductase with ferredoxin reductase and ferredoxin. *Protein Sci.* 2:2112–33

18. Crawford NM. 1995. Nitrate: nutrient and signal for plant growth. *Plant Cell* 7:859–68

19. Crawford NM, Arst HN. 1993. The molecular genetics of nitrate assimilation in fungi and plants. *Annu. Rev. Genet.* 27:115–46

20. Crawford NM, Smith M, Bellissimo D, Davis RW. 1988. Sequence and nitrate regulation of the *Arabidopsis thaliana* mRNA encoding nitrate reductase, a metalloflavoprotein with three functional domains. *Proc. Natl. Acad. Sci. USA* 85:5006–10

21. Dawson HN, Burlingame R, Cannons AC. 1997. Stable transformation of Chlorella: rescue of nitrate reductase-deficient mutants with the nitrate reductase gene. *Curr. Microbiol.* 35:356–62

22. Douglas P, Moorhead G, Hong Y, Morrice N, MacKintosh C. 1998. Purification of a nitrate reductase kinase from *Spinach oleracea* leaves, and its identification as a calmodulin-domain protein kinase. *Planta* 206:435–42

23. Douglas P, Morrice N, MacKintosh C. 1995. Identification of a regulatory phosphorylation site in the hinge 1 region of nitrate reductase from spinach. *Spinacea oleracea* leaves. *FEBS Lett.* 377:113–17

24. Dwivedi UN, Shiraishi N, Campbell WH. 1994. Identification of an "essential" cysteine of nitrate reductase via mutagenesis of its recombinant cytochrome b reductase domain. *J. Biol. Chem.* 269:13785–91

25. Ermler U, Siddiqui RA, Cramm R, Friedrich B. 1995. Crystal structure of the flavohemoglobin from Alcaligenes eutrophus at 1.75 Å resolution. *EMBO J.* 14:6067–77

26. Ferl RJ. 1996. 14-3-3 Proteins and signal transduction. *Annu. Rev. Plant Physiol. Plant Mol. Biol.* 47:49–73

27. Foyer CH, Valadier MH, Migge A, Becker TW. 1998. Drought-induced effects on nitrate reductase activity and mRNA and on the coordination of nitrogen and carbon metabolism in maize leaves. *Plant Physiol.* 117:283–92

28. Garde J, Kinghorn JR, Tomsett AB. 1995. Site-directed mutagenesis of nitrate reductase from *Aspergillus nidulans*. *J. Biol. Chem.* 270:6644–50

29. Garrett RM, Rajagopalan KV. 1996. Site-directed mutagenesis of recombinant sulfite oxidase. *J. Biol. Chem.* 271:7387–91

30. George GN, Garrett RM, Prince RC, Rajagopalan KV. 1996. XAS and EPR spectroscopic studies of site-directed mutants of sulfite oxidase. *J. Am. Chem. Soc.* 118:8588–92

31. Giovannoni G, Land JM, Keir G, Thompson EJ, Heales SJ. 1997. Adaptation of the nitrate reductase and Griess reaction methods for the measurement of serum nitrate plus nitrite levels. *Ann. Clin. Biochem.* 34:193–98

32. Glazier SA, Campbell ER, Campbell WH. 1998. Construction and characterization of nitrate reductase-based amperometric electrode and nitrate assay of fertilizers and drinking water. *Anal. Chem.* 70:1511–15

33. Gonzalez C, Brito N, Marzluf GA. 1995. Functional analysis by site-directed mutagenesis of individual amino acid residues in the flavin domain of *Neurospora crassa* nitrate reductase. *Mol. Gen. Genet.* 249:456–64

34. Granger DL, Taiutor RR, Broockvar KS, Hibbs JB. 1996. Measurement of nitrate and nitrite in biological samples using nitrate reductase and Griess reaction. *Methods Enzymol.* 268:142–51

35. Grisham MB, Johnson GG, Lancaster JR. 1996. Quantitation of nitrate and nitrite in extracellular fluids. *Methods Enzymol.* 268:237–45

36. Hallberg GR. 1989. Nitrate in ground water in the United States. In *Nitrogen Management and Ground Water Protection*, ed. RF Follet, pp. 35–74. Amsterdam: Elsevier

37. Hille R. 1996. The mononuclear molybdenum enzymes. *Chem. Rev.* 96:2757–816

38. Huber JL, Huber SC, Campbell WH, Redinbaugh MG. 1992. Reversible light/dark modulation of spinach leaf nitrate reductase activity involves protein phosphorylation. *Arch. Biochem. Biophys.* 296:58–65

39. Huber SC, Bachmann M, Huber JL. 1996. Post-translation regulation of nitrate reductase activity: a role for Ca^{2+} and 14-3-3 proteins. *Trends Plant Sci.* 1:432–38

40. Hughes RK, Doyle WA, Chovnick A, Whittle JR, Burke JF, et al. 1992. Use of rosy mutant strains of *Drosophila melanogaster* to probe the structure and function of xanthine dehydrogenase. *Biochem. J.* 285:507–13

41. Hurley JH, Chen R, Dean AM. 1996. Determinants of cofactor specificity in isocitrate dehydrogenase: structure of an engineered $ADP^{+} \rightarrow NAD^{+}$ specificity-reversal mutant. *Biochemistry* 35:5670–78

42. Hwang CF, Lin Y, D'Souza T, Cheng CL. 1997. Sequences necessary for nitrate-dependent transcription of Arabidopsis nitrate reductase genes. *Plant Physiol.* 113:853–62

43. Hyde GE, Campbell WH. 1990. High-level expression in *Escherichia coli* of the catalytically active flavin domain of corn leaf NADH:nitrate reductase and its comparison to human NADH:cytochrome b_5 reductase. *Biochem. Biophys. Res. Commun.* 168: 1285–91

44. Hyde GE, Crawford N, Campbell WH. 1991. The sequence of squash NADH:nitrate reductase and its relationship to the sequences of other flavoprotein oxidoreductases: a family of flavoprotein pyridine nucleotide cytochrome reductases. *J. Biol. Chem.* 266:23542–47

45. Hyde GE, Wilberding JA, Meyer AL, Campbell ER, Campbell WH. 1989. Monoclonal antibody-based immunoaffinity chromatography for purifying corn and squash NADH:nitrate reductases. Evidence for an interchain disulfide bond in nitrate reductase. *Plant Mol. Biol.* 13:233–46

46. Ingelman M, Bianchi V, Eklund H. 1997. The three-dimensional structure of flavodoxin reductase from *Escherichia coli* at 1.7 Å resolution. *J. Mol. Biol.* 268:147–57

47. Johnson JL, Bastian NR, Rajagopalan KV. 1990. Molybdopterin guanine dinucleotide: a modified form of molybdopterin identified in the molybdenum cofactor of dimethyl sulfoxide reductase from *Rhodobacter sphaeroides* forma *specialis denitrificans*. *Proc. Natl. Acad. Sci. USA* 87:3190–94

48. Kaiser WM, Brendle-Behnisch E. 1991. Rapid modulation of spinach leaf nitrate reductase activity by photosynthesis. *Plant Physiol.* 96:363–67

49. Karplus PA, Daniels MJ, Herriott JR. 1991. Atomic structure of ferredoxin-NADP$^+$ reductase: prototype for a structurally novel flavoenzyme family. *Science* 251:60–66

50. Kay CJ, Lippay EW. 1992. Mutation of the heme-binding crevice of flavocytochrome b_2 from *Saccharomyces cerevisiae*: altered heme potential and absence of redox cooperativity between heme and FMN centers. *Biochemistry* 31:11376–82

51. Kisker C, Schindelin H, Pacheco A, Wehbi WA, Garrett RM, et al. 1997. Molecular basis of sulfite oxidase deficiency from the structure of sulfite oxidase. *Cell* 91:973–83

52. LaBrie ST, Crawford NM. 1994. A glycine to aspartic acid change in the MoCo domain of nitrate reductase reduces both activity and phosphorylation levels in Arabidopsis. *J. Biol. Chem.* 269:14497–501

53. Lejay L, Quillere I, Roux Y, Tillard P, Cliquet J-B, et al. 1997. Abolition of posttranscriptional regulation of nitrate reductase partially prevents the decrease in leaf NO_3^- reduction when photosynthesis is inhibited by CO_2 deprivation, but not in darkness. *Plant Physiol.* 115:623–30

54. Lindqvist Y, Lu G, Schneider G, Campbell WH. 1997. Crystallographic studies of the FAD/NADH binding fragment of corn nitrate reductase. See Ref. 94a, pp. 899–907

55. Liu D, Bienkowska J, Petosa C, Collier RJ, Fu H, et al. 1995. Crystal structure of the zeta isoform of the 14-3-3 protein. *Nature* 376:191–94

56. Lu G, Campbell WH, Schneider G, Lindqvist Y. 1994. Crystal structure of the FAD-containing fragment of corn nitrate reductase at 2.5 Å resolution: relationship to other flavoprotein reductases. *Structure* 2:809–21

57. Lu G, Lindqvist Y, Schneider G, Dwivedi UN, Campbell WH. 1995. Structural studies on corn nitrate reductase. Refined structure of the cytochrome b reductase fragment at 2.5 Å, its ADP complex and an active site mutant and modeling of the cytochrome b domain. *J. Mol. Biol.* 248:931–48

58. MacKintosh C. 1992. Regulation of spinach-leaf nitrate reductase by reversible phosphorylation. *Biochim. Biophys. Acta* 1137:121–26

59. Mathews FS, Levine M, Argos P. 1971. The structure of calf liver cytochrome b_5 at 2.8 Å resolution. *Nat. New Biol.* 233:15–16

60. Matson PA, Naylor R, Ortiz-Monasterio I. 1998. Integration of environmental, agronomic and economic aspects of fertilizer management. *Science* 280:112–15

61. Mellor RB, Ronnenberg J, Campbell WH, Diekmann S. 1992. Reduction of nitrate and nitrite in water by immobilized enzymes. *Nature* 355:717–19

62. Mendel RR. 1997. Molybdenum cofactor of higher plants: biosynthesis and molecular biology. *Planta* 203:399–405

63. Meyer C, Levin JM, Roussel J-M, Rouze

P. 1991. Mutational and structural analysis of the nitrate reductase heme domain of *Nicotiana plumbaginifolia*. *J. Biol. Chem.* 266:20561–66

64. Mittl PR, Berry A, Scrutton NS, Perham RN, Schulz GE. 1993. Structural differences between wild-type NADP-dependent glutathione reductase from *Escherichia coli* and a redesigned NAD-dependent mutant. *J. Mol. Biol.* 231:191–95

65. Moorhead G, Douglas P, Morrice N, Scarable M, Aitken A, et al. 1996. Phosphorylated nitrate reductase from spinach leaves is inhibited by 14-3-3 proteins and activated by fusicoccin. *Curr. Biol.* 6:1104–13

66. Nishida H, Inaka K, Yamanaka M, Kaida S, Kobayashi K, et al. 1995. Crystal structure of NADH-cytochrome b_5 reductase from pig liver at 2.4 Å resolution. *Biochemistry* 34:2763–67

67. Nolan BT, Ruddy BC. 1996. *Nitrate in the ground waters of the United States—assessing the risk.* U.S. Geol. Surv. Fact Sheet FS-092–96 (http://wwwrvares.er.usgs.gov/nawqa/fs-092–96/fs-0092–96main.html)

68. Nussaume L, Vincentz M, Meyer C, Boutin J-P, Caboche M. 1995. Post-transcriptional regulation of nitrate reductase by light is abolished by an N-terminal deletion. *Plant Cell* 7:611–21

69. Pang XP, Gupta SC, Moncrief JF, Rosen CJ, Cheng HH. 1998. Evaluation of nitrate leaching potential in Minnesota glacial outwash soils using the CERES-maize model. *J. Environ. Qual.* 27:75–85

70. Pelley J. 1998. What is causing toxic algal blooms. *Environ. Sci. Technol.* 32: A26–30

71. Petosa C, Masters SC, Bankston LA, Pohl J, Wang B, et al. 1998. 14-3-3 zeta binds a phosphorylated Raf peptide and an unphosphorylated peptide via its conserved amphipathic groove. *J. Biol. Chem.* 273:16305–10

72. Puckett LJ. 1995. Identifying the major sources of nutrient water pollution. *Environ. Sci. Technol.* 29:408A–14A

73. Quinn GB, Trimboli AJ, Barber MJ. 1994. Construction and expression of a flavocytochrome b_5 chimera. *J. Biol. Chem.* 269:13375–81

74. Quinn GB, Trimboli AJ, Prosser IM, Barber MJ. 1996. Spectroscopic and kinetic properties of a recombinant form of the flavin domain of spinach NADH:nitrate reductase. *Arch. Biochem. Biophys.* 327:151–60

75. Ratnam K, Shiraishi N, Campbell WH, Hille R. 1995. Spectroscopic and kinetic characterization of the recombinant wild-type and C242S mutant of the cytochrome b reductase fragment of nitrate reductase. *J. Biol. Chem.* 270: 24067–72

76. Ratnam K, Shiraishi N, Campbell WH, Hille R. 1997. Spectroscopic and kinetic characterization of the recombinant cytochrome c reductase fragment of nitrate reductase: identification of the rate limiting catalytic step. *J. Biol. Chem.* 272:2122–28

77. Redinbaugh MG, Campbell WH. 1985. Quaternary structure and composition of squash NADH:nitrate reductase. *J. Biol. Chem.* 260:3380–85

78. Redinbaugh MG, Campbell WH. 1991. Higher plant responses to environmental nitrate. *Physiol. Plant.* 82:640–50

79. Reid LS, Taniguchi VT, Gray HB, Mauk AG. 1982. Oxidation-reduction equilibrium of cytochrome b_5. *J. Am. Chem. Soc.* 104:7516–19

80. Rossmann MG, Mora D, Olsen KW. 1974. Chemical and biological evolution of a nucleotide-binding protein. *Nature* 250:194–99

81. Rouze P, Caboche M. 1992. Nitrate reduction in higher plants: molecular approaches to function and regulation. In *Inducible Plant Proteins*, ed. JL Wray, pp. 45–77. Cambridge, MA: Cambridge Univ. Press

82. Scheible WR, Gonzalez-Fontes A, Morcuende R, Lauerer M, Geiger M, et al. 1997. Tobacco mutants with a decreased number of functional nia genes compensate by modifying the diurnal regulation of transcription, post-translational modification and turnover of nitrate reductase. *Planta* 203:304–19

83. Scheible WR, Gonzalez-Fontes A, Morcuende R, Lauerer M, Muller-Rober B, et al. 1997. Nitrate acts as a signal to induce organic acid metabolism and repress starch metabolism in tobacco. *Plant Cell* 9:783–98

84. Scheible WR, Lauerer M, Schulze ED, Caboche M, Stitt M. 1997. Accumulation of nitrate in the shoot acts as signal to regulate shoot-root allocation in tobacco. *Plant J.* 11:671–91

85. Schondorf T, Hachtel W. 1995. The choice of reducing substrate is altered by replacement of an alanine by a proline in the FAD domain of a bispecific NAD(P)H-nitrate reductase from birch. *Plant Physiol.* 108:203–10

86. Scrutton NS, Berry A, Perham RN.

1990. Redesign of the coenzyme specificity of a dehydrogenase by protein engineering. *Nature* 343:38–43

87. Sehnke PC, Ferl RJ. 1996. Plant metabolism: enzyme regulation by 14-3-3 proteins. *Curr. Biol.* 6:1403–5

88. Serre L, Vellieux FM, Medina M, Gomez-Moreno C, Fontecilla-Camps JC, et al. 1996. X-ray structure of the ferredoxin:NADP$^+$ reductase from the cyanobacterium Anabaena PCC 7119 at 1.8 Å resolution, and crystallographic studies of NADP$^+$ binding at 2.25 Å resolution. *J. Mol. Biol.* 263:20–39

89. Shaffer MJ, Halvorson AD, Pierce FJ. 1991. Nitrate leaching and economic analysis package (NLEAP): model description and applications. In *Managing Nitrogen for Groundwater Quality and Farm Productivity*, ed. RF Follett, DR Keeney, RM Cruse, pp. 285–322. Madison, WI: Soil Sci. Soc. Am.

90. Shiraishi N, Campbell WH. 1997. Expression of nitrate reductase FAD-containing fragments in Pichia. See Ref. 94a, pp. 931–34

91. Shiraishi N, Croy C, Kaur J, Campbell WH. 1998. Engineering of pyridine nucleotide specificity of nitrate reductase: mutagenesis of recombinant cytochrome b reductase fragment of *Neurospora crassa* NADPH:nitrate reductase. *Arch. Biochem. Biophys.* 358: 104–15

92. Smil V. 1997. Global population and the nitrogen cycle. *Sci. Am.* 277:76–81

93. Solomonson LP, Barber MJ. 1989. Algal nitrate reductases. See Ref. 102a, pp. 123–54

94. Solomonson LP, Barber MJ. 1990. Assimilatory nitrate reductase: functional properties and regulation. *Annu. Rev. Plant Physiol. Plant Mol. Biol.* 41:225–53

94a. Stevenson KJ, ed. 1996. *Flavins and Flavoproteins*. Calgary, Can: Univ. Calgary Press

95. Su W, Huber SC, Crawford NM. 1996. Identification in vitro of a posttranslational regulatory site in the hinge

1 region of Arabidopsis nitrate reductase. *Plant Cell* 8:519–27

96. Su W, Mertens JA, Kanamaru K, Campbell WH, Crawford NM. 1997. Analysis of wild-type and mutant plant nitrate reductase expressed in the methylotrophic yeast *Pichia pastoris*. *Plant Physiol.* 115:1135–43

97. Trimboli AJ, Barber MJ. 1994. Assimilatory nitrate reductase: reduction and inhibition by NADH/NAD$^+$ analogs. *Arch. Biochem. Biophys.* 315:48–53

98. Trimboli AJ, Quinn GB, Smith ET, Barber MJ. 1996. Thiol modification and site-directed mutagenesis of the flavin domain of spinach NADH:nitrate reductase. *Arch. Biochem. Biophys.* 331:117–26

99. Tsay YF, Schroeder JI, Feldmann KA, Crawford NM. 1993. The herbicide sensitivity gene CHL1 of Arabidopsis encodes a nitrate-inducible nitrate transporter. *Cell* 72:705–13

100. Vitousek PM, Mooney HA, Lubchenco J, Melillo JM. 1997. Human domination of Earth's ecosystems. *Science* 277:494–99

101. Wang M, Roberts DL, Paschke R, Shea TM, Masters BS, et al. 1997. Three-dimensional structure of NADPH-cytochrome P450 reductase: prototype for FMN- and FAD-containing enzymes. *Proc. Natl. Acad. Sci. USA* 94: 8411–16

102. Wei X, Ming LJ, Cannons AC, Solomonson LP. 1998. 1H and 13C NMR studies of a truncated heme domain from *Chlorella vulgaris* nitrate reductase: signal assignment of the heme moiety. *Biochim. Biophys. Acta* 1382:129–36

102a. Wray J, Kinghorn J, eds. 1989. *Molecular and Genetic Aspects of Nitrate Assimilation*. New York: Oxford Univ. Press

103. Xiao B, Smerdon SJ, Jones DH, Dodson GG, Soneji Y, et al. 1995. Structure of a 14-3-3 protein and implications for coordination of multiple signaling pathways. *Nature* 376:188–91
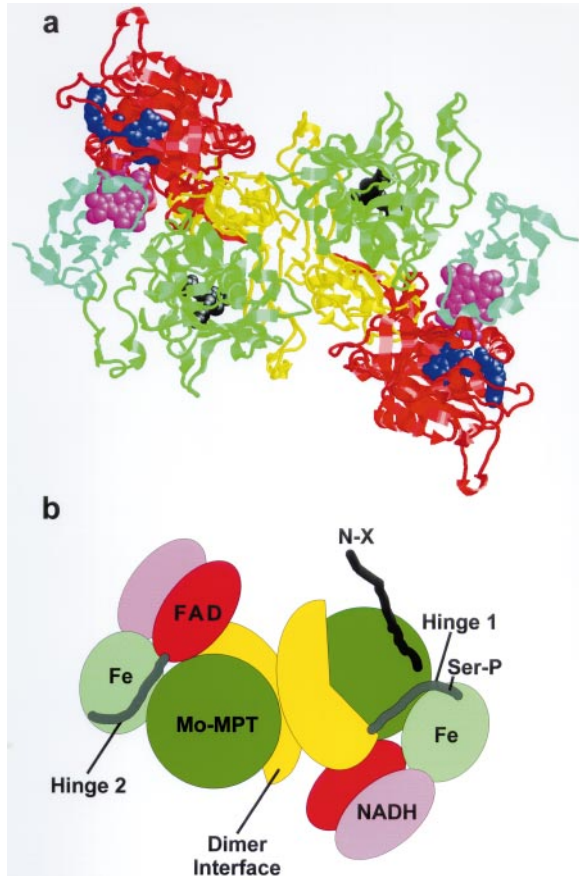
Figure 3 "Working model" for the three-dimensional structure of the holonitrate reductase ho-
modimer. (*a*) Ribbon-model rendering of dimeric nitrate reductase with coordinates derived from
docking two cytochrome c reductase fragments (57) on an atom replacement model of the dimer of
Arabidopsis NIA2 (residues 91 to 490) generated from sulfite oxidase A and B chains [51; 1SOX
in PDB (Protein Data Base)]. (*b*) Schematic model of nitrate reductase dimer. From the blocked N
terminus *(N-X)*, the order of domains and hinge regions are: N-terminal region *(black tube)**; Mo-
molybdopterin *(Mo-MPT)* domain *(dark green with Mo-MPT black)*; interface domain *(yellow)*;
Hinge 1 *(gray tube with phosphorylated Ser534)**; cytochrome b domain *(light green with heme-Fe
purple)*; Hinge 2 *(gray tube)**; cytochrome b reductase fragment [in (*a*) *red* with FAD *blue*; in (*b*)
FAD domain *red* and *NADH domain pink*]. Asterisked regions are not included in (*a*).